Atomic-Scale Desorption Through Electronic and Vibrational Excitation Mechanisms

T.-C. Shen,* C. Wang, G. C. Abeln, J. R. Tucker, J. W. Lyding, Ph. Avouris,* R. E. Walkup

The scanning tunneling microscope has been used to desorb hydrogen from hydrogen-terminated silicon (100) surfaces. As a result of control of the dose of incident electrons, a countable number of desorption sites can be created and the yield and cross section are thereby obtained. Two distinct desorption mechanisms are observed: (i) direct electronic excitation of the Si–H bond by field-emitted electrons and (ii) an atomic resolution mechanism that involves multiple-vibrational excitation by tunneling electrons at low applied voltages. This vibrational heating effect offers significant potential for controlling surface reactions involving adsorbed individual atoms and molecules.

The scanning tunneling microscope (STM) has been used to manipulate materials on the atomic and nanometer scales. A number of approaches have made use of direct tip-sample interactions, strong electric fields, or electronic excitation (*1–3*). Here we explore atomic desorption processes from the 2×1 and 3×1 hydride phases of the hydrogen-exposed Si(100)-(2×1) surface induced by field-emitted or tunneling electrons from the STM tip. We delineate two distinct mechanisms: (i) direct electronic excitation of the Si–H bond by electrons field-emitted from the STM tip and (ii) an excitation mechanism in which inelastic electron tunneling induces multiple-vibrational excitation of the Si–H bond leading to hydrogen desorption.

Desorption induced by electronic transitions (DIET) has been a very active research area (*4, 5*). Because of the difficulty of detecting small numbers of neutral species, most work on DIET has focused on the desorption of positive ions (*4, 5*), although these are usually minority species. We show here that performing DIET with the STM has a number of advantages. First, desorption by STM is detected in terms of changes in the STM image that result from alterations in the local electronic structure, in this case from the appearance of new dangling bonds. Thus, STM-stimulated DIET is capable of single-atom detection independent of the charge state of the desorbed species. Second, any site selectivity of the desorption process can be detected directly with the STM. Third, there is significant interest in understanding and controlling DIET processes with the STM that can be used for lithography and materials modification on the nanometer (*6*) and even on the atomic scale (*7*). Finally, there is interest in the possibility of utilizing a new excitation mechanism involving multiple-vibrational excitation.

The feasibility of using field-emitted electrons from an STM tip to bring about hydrogen desorption was first demonstrated for hydrogen adsorbed on Si(111) by Becker *et al.* (*8*). The resolution of STM desorption at energies sufficiently high to induce electronic excitation (field-emission regime) is limited to dimensions ~5 nm by the relatively large distance between the tip and the sample and by tip geometry. In contrast, better, atomic-scale control of the desorption process should be possible in the tunneling règime with a vibrational excitation mechanism. Model calculations have indicated that the extremely high current densities present in the STM can produce multiple-vibrational excitation through inelastic electron tunneling, and in some cases the deposited energy can be sufficiently high to cause desorption (*9, 10*). The amount of vibrational energy depends critically on the vibrational lifetime, which, in turn, depends on the nature of the substrate. For example, the vibrational lifetime of hydrogen adsorbed on a metal is extremely short (~10^{-12} s) (*11*), whereas hydrogen on silicon has a very long lifetime: ~10^{-9} s on Si(111) (*12*) and ~10^{-8} s on Si(100) (*13*). In systems with long lifetimes such as H on Si, we would expect more efficient vibrational excitation (*9*). The results presented in this report establish the existence of this vibrational desorption mechanism. The ability of the tunneling current of the STM to deposit significant amounts of vibrational energy in adsorbates, under appropriate conditions, can have important implications for STM studies of surface dynamical processes. In terms of materials manipulation, desorption induced by the STM operating in the tunneling regime makes atomic-scale control possible.

All experiments were performed under ultrahigh vacuum conditions (base pressure <1 × 10^{-10} torr). The Si(100) samples were As-doped (0.005 ohm·cm) or B-doped (0.1 ohm·cm) wafers. In situ preparation of H-terminated 2×1 and 3×1 Si(100) surfaces has been described in detail elsewhere (*7, 14, 15*). The STM desorption experiments were carried out at room temperature under constant-current feedback control.

An STM image of the occupied states of an H-terminated Si(100)-(2×1) surface (sample bias $V_s = -1.3$ V) (Fig. 1A) shows rows of H-terminated Si dimers. We induced desorption by raising the sample bias to +8 V. Three low-density lines (see arrows) of H-desorption sites (that is, Si dangling bonds) were written at 1000 Å/s (Fig. 1B). High-resolution images of the unoccupied states (Fig. 2) allow both Si atoms in each Si dimer to be imaged. Figure 2 shows

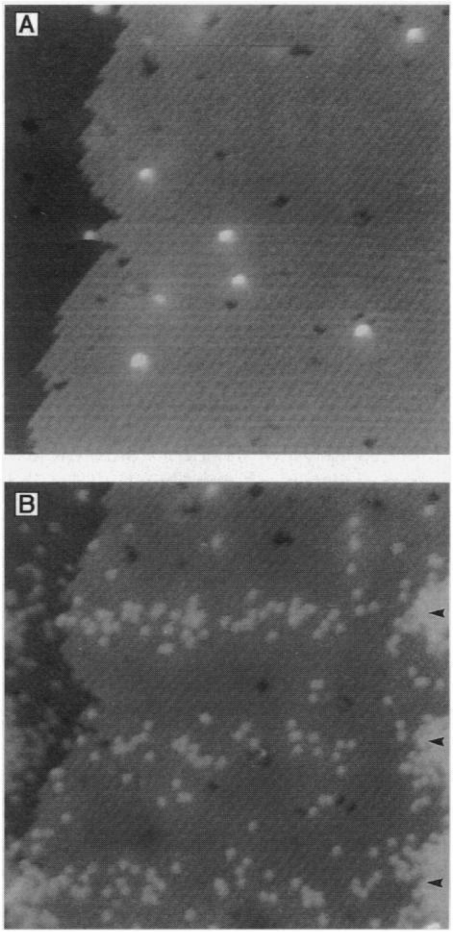

Fig. 1. (**A**) An STM image of the occupied states of a 200 Å by 200 Å area of a Si(100)-2×1:H surface (As-doped, 0.005 ohm·cm). (**B**) The same surface after three horizontal lines (indicated by arrows) of Si dangling bonds (bright spots) were formed through hydrogen desorption at a sample bias V_s = +8 V and a current I = 0.01 nA. The line electron dose was $Q = 1 \times 10^{-6}$ C/cm. Both images were recorded at $V_s = -1.3$ V and I = 0.1 nA.

T.-C. Shen, C. Wang, G. C. Abeln, J. R. Tucker, J. W. Lyding, Department of Electrical and Computer Engineering and Beckman Institute, University of Illinois at Urbana-Champaign, Urbana, IL 61801, USA.
Ph. Avouris and R. E. Walkup, IBM Research Division, T. J. Watson Research Center, Yorktown Heights, NY 10598, USA.

*To whom correspondence should be addressed.

that electronic desorption produces dangling bonds (bright spots) on one of the two Si atoms of an individual Si dimer; that is, excitation leads to the desorption of individual H atoms. Whereas the Si(100)-2×1:H surface has only one kind of H adsorption site, the 3×1 phase has alternating monohydride (Si–H) and dihydride (SiH_2) sites (*14*). Our experiments indicate that there is a site selectivity in this case, with desorption occurring preferentially at monohydride sites.

From the number of desorption sites and the total number of incident electrons, the desorption yield and cross section can be determined. The dependence of the desorption yield on applied voltage (Fig. 3) shows a threshold at a sample bias of roughly +6.5 V in the field-emission regime (*n*-type samples). This threshold is consistent with electron energy loss spectra of Si(100)-2×1:H (*16*) in which a transition with maximum at ~8 eV and onset at ~6 eV were observed and interpreted as an electronic excitation of the Si–H group. This assignment was further supported by calculations (*17*), which identified it with the σ(Si–H) bonding to σ*(Si–H) antibonding transition. The free Si–H molecule also has broad dissociative transitions within this same energy range (*18*).

When the energy of incident electrons is greater than the threshold energy (~6.5 V), the yield is nearly constant at $\sim 2.4 \times 10^{-6}$ H atoms per electron and independent of both voltage and current. The cross section is 4×10^{-21} cm^2, obtained by dividing the yield by the surface H atom density. When the energy of incident electrons falls below the electronic threshold energy, desorption does not cease but becomes several orders of magnitude smaller and is strongly dependent on current and voltage (Fig. 4). Apparently, a different desorption mechanism now operates. The strong dependence on current indicates that many electrons must be involved in the excitation-desorption process.

Inelastic electron tunneling in the STM can lead to vibrational excitation of an adsorbate. Two different mechanisms by which this excitation can take place have been discussed (*19*). In the dipole excitation mechanism, the field produced by an incident electron interacts with the transition dipole moment μ of the vibrational mode. When there is sufficient energy to excite the vibration, the ratio of inelastic to elastic tunneling, f_{in}, is independent of the electron energy but depends on μ (*19*). The resonance excitation mechanism, on the other hand, involves temporary trapping of the electron in an unoccupied or partially occupied adsorbate level (resonance). In this case, the excitation probability is energy-dependent and roughly proportional to the density of states of the resonance evaluated at the Fermi energy of the tip (*19*).

The degree of vibrational heating induced by the STM depends on a balance between vibrational excitation and relaxation processes. Electrons excite Si–H vibrational transitions with a rate proportional to the tunneling current, and vibrational energy is lost by coupling to phonons. A useful zero-order description of desorption through multiple-vibrational excitation can be obtained if one regards Si–H as a truncated harmonic oscillator (*20*). The steady-state solution of the master equations that govern the population of the oscillator levels is then $p_n \sim (u/d)^n = \exp(-n\hbar\omega/kT_{vib})$, where u and d are the net upward and downward transition rates, n is the vibrational quantum number, $\hbar$ is Planck's constant divided by 2π, ω is the angular vibrational frequency, and k is Boltzmann's constant. One can characterize this distribution with an effective vibrational temperature $kT_{vib} = \hbar\omega/\ln(d/u)$. Desorption within this model proceeds with a rate (*9*)

$$R \simeq \left(\gamma f_T \frac{\Delta E}{\hbar\omega}\right) e^{-\Delta E/kT_{vib}}$$

Here γ is the vibrational decay, or relaxation, rate, ΔE is the energy barrier that needs to be surmounted, and f_T is the probability that an atom with energy above the barrier will desorb. Using appropriate values for the Si–H vibrational energy ($\hbar\omega = 0.25$ eV) (*21*), relaxation rate ($\gamma \sim 1 \times 10^8$ s^{-1}) (*13*), and barrier height ($\Delta E = 3.0$ eV) (*9*), the model predicts desorption rates within the experimental range for inelastic tunneling fractions of $f_{in} \sim 10^{-3}$. This is the expected order of magnitude for inelastic tunneling by means of either dipole or resonance mechanisms (*22*). Thus, these simple estimates of current-induced desorption support the mechanism of multiple-vibrational excitation.

The experimental data in Fig. 4 show a dependence of the desorption yield not only on the tunneling current but also on the voltage (V_s). The voltage dependence could, in principle, reflect either a varying electric field between tip and sample or an energy dependence of the excitation cross section. The electric field can be estimated as V_s/z, where z is the tip-sample distance. In this way we find that the field strength does not vary significantly with voltage under the constant-current conditions used in the experiments. Thus, although the electric field is important in other respects, such as localizing the Si–H excitation under the tip by shifting its energy, it is not the likely cause of the voltage dependence. More likely, the dependence of the desorption yield on V_s reflects an energy dependence of the excitation cross section. For the dipole excitation mechanism, no energy dependence is expected (*19*), and $f_{in} \sim 8 \times 10^{-4}$ is estimated

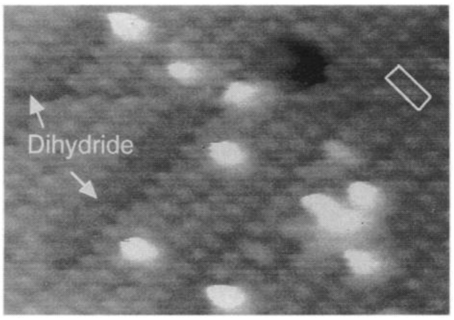

Fig. 2. An STM image of the unoccupied states of an area (100 Å by 100 Å) of a Si(100)-(2×1):H surface (V_s = +1.5 V, I = 0.1 nA). Hydrogen has been desorbed at V_s = +5.5 V (I = 0.1 nA, Q = 1 × 10^{-6} C/cm). A (2×1) surface unit cell is outlined. The bright features are single Si atom dangling bonds produced by hydrogen desorption.

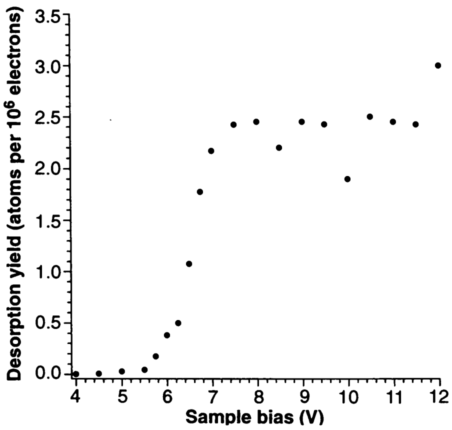

Fig. 3. Hydrogen desorption yield, obtained by counting the number of desorbed H atoms divided by the total number of incident electrons, as a function of the sample bias voltage for an As-doped sample.

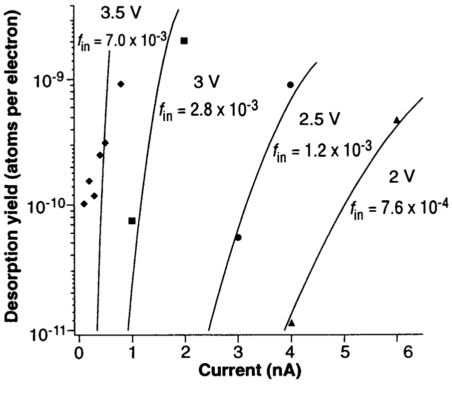

Fig. 4. Hydrogen desorption yields at incident electron energies (bias voltages) less than the electronic threshold energy. The curves shown are the predictions of the desorption model involving multiple-vibrational excitation. The inelastic fractions f_{in} resulting from fitting to the data are shown next to the curves.

from spectral data. Excitation through a resonance level, however, should be energy-dependent (*19*). Electronic structure calculations (*17*, *23*) and experiments (*24*, *25*) point to the onset of a σ^*(Si–H) empty level in the relevant energy range, roughly 2 to 3 eV above the Fermi level. The inelastic fractions that quantitatively account for the experimental observations, as indicated in Fig. 4, are in rough agreement with expectations based on the profile of this resonance. We thus conclude that the H atom desorption mechanism in the energy range from about 2 to 5 eV can be described as resonantly enhanced multiple-vibrational excitation.

The use of tunneling electrons in place of field-emitted electrons to desorb H atoms makes possible STM lithography with atomic resolution. An example involving a pattern of parallel lines at 30 Å pitch written with $V_s = +3$ V is shown in Fig. 5. The lines are, for the most part, composed of single Si atom dangling bonds or Si dimer dangling bonds corresponding to a resolution of <10 Å. Figure 5 shows that the vibrational mechanism can lead to single H atom desorption. However, because of their close proximity and the high current densities utilized, often both H atoms on a single dimer are desorbed (see arrows).

Dangling bond patterns such as that in Fig. 5 can be converted to chemical modification patterns if the selectively depassivated surface is exposed to reactive gases (*7*). Vibrational excitation of adsorbates with atomic resolution opens up many other possibilities for selective activation, either directly or through subsequent energy transfer to other degrees of freedom, of processes such as adsorbate dissociation, bimolecular reaction, and diffusion (*26*).

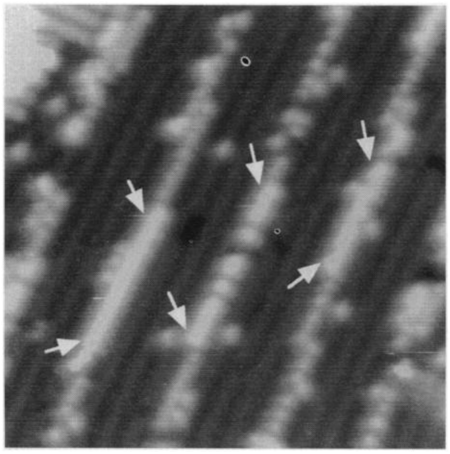

Fig. 5. An STM image (150 Å by 150 Å, $V_s = -1.4$ V, $I = 0.1$ nA) showing a pattern of 30 Å pitch lines of dangling bonds written with $V_s = +3$ V, $I = 4.5$ nA, and $Q = 6 \times 10^{-4}$ C/cm. The arrows point to sites at which both H atoms of an Si dimer have been desorbed.

REFERENCES AND NOTES

1. Ph. Avouris, Ed., *Atomic and Nanometer Scale Modification of Materials: Fundamentals and Applications* (Kluwer, Dordrecht, Netherlands, 1993).
2. C. A. Quate, in *Highlights in Condensed Matter Physics*, L. Esaki, Ed. (Plenum, New York, 1991), pp. 573–630.
3. J. A. Stroscio and D. M. Eigler, *Science* **254**, 1319 (1991).
4. R. D. Ramsier and J. T. Yates Jr., *Surf. Sci. Rep.* **12**, 243 (1991).
5. Ph. Avouris and R. E. Walkup, *Annu. Rev. Phys. Chem.* **40**, 173 (1989).
6. E. S. Snow and P. M. Cambell, *Appl. Phys. Lett.* **64**, 1932 (1994).
7. J. W. Lyding, T.-C. Shen, J. S. Hubacek, J. R. Tucker, G. C. Abeln, *ibid.*, p. 2010.
8. R. S. Becker, G. S. Higashi, Y. J. Chabal, A. J. Becker, *Phys. Rev. Lett.* **65**, 1917 (1990).
9. R. E. Walkup, D. M. Newns, Ph. Avouris, in (*1*), pp. 97–109.
10. ———, *Phys. Rev. B* **48**, 1858 (1993).
11. B. N. J. Persson, *ibid.* **44**, 3277 (1991).
12. P. Guyot-Sionnest, P. Dumas, Y. J. Chabal, G. S. Higashi, *Phys. Rev. Lett.* **64**, 2156 (1990).
13. P. Guyot-Sionnest, P. H. Lin, E. M. Miller, *J. Chem. Phys.*, **102**, 4269 (1995).
14. J. J. Boland, *Surf. Sci.* **261**, 17 (1992).
15. D. T. Jiang, G. W. Anderson, K. Griffiths, T. K. Sham, P. R. Norton, *Phys. Rev. B* **48**, 4952 (1993).
16. S. Maruno, H. Iwasaki, K. Horioka, S.-T. Li, S. Nakamura, *ibid.* **27**, 4110 (1983).
17. S. Ciraci, R. Butz, E. M. Oelling, H. Wagner, *ibid.* **30**, 711 (1984).
18. K. P. Huber and G. Herzberg, *Molecular Spectra and Molecular Structure* (Van Nostrand Reinhold, New York, 1979).
19. B. N. J. Persson, *Phys. Scr.* **38**, 282 (1988).
20. N. G. van Kempen, *Stochastic Processes in Physics and Chemistry* (North-Holland, Amsterdam, 1981).
21. Y. J. Chabal and K. Raghavachari, *Phys. Rev. Lett.* **53**, 282 (1984).
22. B. N. J. Persson and A. Baratoff, *ibid.* **59**, 339 (1987).
23. M. Schlüter and M. L. Cohen, *Phys. Rev. B* **17**, 716 (1978).
24. L. S. O. Johansson, R. I. G. Uhrberg, G. V. Hansson, *ibid.* **38**, 13490 (1988).
25. J. Wintterlin and Ph. Avouris, *J. Chem. Phys.* **100**, 687 (1994).
26. Ph. Avouris, *Acc. Chem. Res.* **28**, 95 (1995).

27. This work is supported by an Office of Naval Research University Research Initiative under grant N00014-92-J-1519. We acknowledge valuable discussions with P. von Allmen (T.-C.S.), B. N. J. Persson (Ph.A.), and P. Guyot-Sionnest (Ph.A.). We thank T. M. Jackman, who provided valuable help with graphics.

25 January 1995; accepted 28 March 1995

Polystyrene-Dendrimer Amphiphilic Block Copolymers with a Generation-Dependent Aggregation

J. C. M. van Hest, D. A. P. Delnoye, M. W. P. L. Baars,
M. H. P. van Genderen, E. W. Meijer*

A class of amphiphilic macromolecules has been synthesized by combining well-defined polystyrene (PS) with poly(propylene imine) dendrimers. Five different generations, from PS-*dendr*-NH_2 up to PS-*dendr*-$(NH_2)_{32}$, were prepared in yields of 70 to 90 percent. Dynamic light scattering, conductivity measurements, and transmission electron microscopy show that in aqueous phases, PS-*dendr*-$(NH_2)_{32}$ forms spherical micelles, PS-*dendr*-$(NH_2)_{16}$ forms micellar rods, and PS-*dendr*-$(NH_2)_8$ forms vesicular structures. The lower generations of this class of macromolecules show inverted micellar behavior. The observed effect of amphiphile geometry on aggregation behavior is in qualitative agreement with the theory of Israelachvili *et al.* The amphiphiles presented here are similar in shape but different in size as compared with traditional surfactants, whereas they are similar in size but different in shape as compared with traditional block copolymers.

The synthesis and characterization of new amphiphilic structures is one of the most daring and promising approaches toward a better understanding of the structure-property relation of amphiphiles (*1*). Historically, the field has been subdivided into traditional surfactants and amphiphilic block copolymers. Both classes have been subjected to extensive studies (*2*–*4*), but a detailed comparison between surfactants and block copolymers that would make it possible to understand the effect of increasing size and shape on aggregation has not been possible, because of distinct differences in the polar segments. The low–molecular weight surfactants have a compact polar head group, whereas the block copolymers known thus far have linear, extendable polar chains.

Recently, dendrimers, which are well-defined and highly branched macromolecules that emanate from a central core, have begun to receive scientific attention (*5*). These spherical structures have been proposed as precise nanoscopic building blocks (*6*). New architectures have been synthesized (*7*), including unimolecular micelles and structures containing dendrimers and linear macromolecules (*8*). Chapman *et al.* (*9*) presented hydra-amphiphiles that

---

Laboratory of Organic Chemistry, Eindhoven University of Technology, Post Office Box 513, 5600 MB Eindhoven, Netherlands.

*To whom correspondence should be addressed.